BMC Nephrology

RESEARCH Open Access

P4HB regulates the TGFβ/SMAD3 signaling pathway through PRMT1 to participate in high glucose-induced epithelial-mesenchymal transition and fibrosis of renal tubular epithelial cells

Haifeng Wang[1], Yang Li[2], Na Wu[2], Chunmei Lv[2] and Yishu Wang[2*]

Abstract

Background Diabetic nephropathy (DN) is a common complication of diabetes mellitus, and Prolyl 4-Hydroxylase Subunit Beta (P4HB) expression is increased in high glucose (HG)-induced renal tubular epithelial cells (TECs). But it's role in HG-induced TECs remains to be elucidated.

Methods The HK-2 cells were induced using HG and transfected with SiRNA-P4HB. DCFH-DA staining was utilized for the detection of cellular levels of ROS. WB and immunofluorescence were utilized to detect the expression of P4HB, epithelial-mesenchymal transition (EMT), fibrosis, and TGFβ/SMAD3-related proteins in HK-2 cells. Online databases were utilized for predicting the interaction target of P4HB, and immunoprecipitation (IP) experiments were employed to validate the binding of P4HB with the target. SiRNA and overexpression vectors of target gene were used to verify the mechanism of action of P4HB.

Results HG induced an increase in the expression of P4HB and TGFβ, p-SMAD3, and ROS in HK-2 cells. Furthermore, HG downregulated the expression of E-cadherin and upregulated the expression of N-cadherin, Vimentin, α-SMA, Fibronectin, Collagen IV, SNAIL, and SLUG in HK-2 cells. Interfering with P4HB significantly reversed the expression of these proteins. Database predictions and IP experiments showed that P4HB interacts with PRMT1, and the expression of PRMT1 was increased in HG-induced HK-2 cells. Interfering with PRMT1 inhibited the changes in expression of EMT and fibrosis related proteins induced by HG. However, overexpression of PRMT1 weakened the regulatory effect of P4HB interference on the EMT, fibrosis, and TGFβ/SMAD3-related proteins in HK-2 cells.

Conclusion P4HB regulated the TGFβ/SMAD3 signaling pathway through PRMT1 and thus participates in HG-induced EMT and fibrosis in HK-2 cells.

Keywords High glucose, Renal tubular epithelial cells, P4HB, Epithelial-mesenchymal transition, Fibrosis

*Correspondence:
Yishu Wang
WangYSDocdoc@163.com

[1]Department of nephrology, China-Japan Friendship Hospital, chaoyang District, 100029 Beijing, China
[2]Comprehensive Internal Medicine Department, Beijing Xiaotangshan Hospital, Xiaotangshan Town, Changping District, 102211 Beijing, China

Introduction

Diabetic nephropathy (DN), resulting from diabetes, is a leading factor in global end-stage renal disease [1], simultaneously ranking among the primary causes of mortality in diabetes [2]. About half of individuals with type 2 diabetes (T2D) and one-third of those with type 1 diabetes (T1D) exhibit signs of DN [3]. The progression of DN is multifaceted, encompassing factors like disruptions in oxygen and glucose metabolism [4]. DN is marked by enduring albuminuria resulting from renal interstitial fibrosis, stemming from high glucose (HG)-induced epithelial-mesenchymal transition (EMT) and tubular fibrosis [5, 6]. Therefore, mitigating HG-induced EMT and tubular fibrosis bears significant importance in curbing diabetic nephropathy.

Fibrosis manifests in numerous chronic inflammatory conditions, including diabetic nephropathy [7]. The defining feature is the unregulated buildup of extracellular matrix (ECM) elements like collagen and fibronectin, resulting in organ dysfunction [8]. The transforming growth factor (TGF)-β acts as a key regulator in both physiological and pathological fibrosis [9], mainly mediated via the classical SMAD3 signaling pathway [10]. Current research suggests that the activation of the TGF-β/SMAD3 pathway participates in HG-induced EMT and fibrosis in renal tubular epithelial cells [11]. Following this, activated by TGF-β, downstream SMAD3 transcriptionally activates Snail Family Transcriptional Repressor 1 (SNAIL), Snail Family Transcriptional Repressor 2 (SLUG), and other EMT transcription factors, ultimately leading to EMT and fibrosis [12].

Prolyl 4-Hydroxylase Subunit Beta (P4HB) is a crucial gene that facilitates collagen maturation and plays a role in promoting EMT and hepatic fibrosis [13, 14]. Investigations reveal an increased expression of P4HB in renal tubular epithelial cells induced by HG [15], but its specific role in these cells during HG induction remains unclear. This study employs online database prediction and validation to elucidate the potential interaction between P4HB and Protein Arginine Methyltransferase-1 (PRMT1). Research shows an upregulation of PRMT1 expression in the serum of DN patients and in the renal tissues of DN mice [16], demonstrating its capability to activate the TGFβ/SMAD2/3 signaling pathway [17].

Therefore, the aim of this study was to investigate whether P4HB could modulate the TGFβ/SMAD signal by interacting with PRMT1, thus playing a role in HG-induced EMT and fibrosis in renal tubular epithelial cells. And provides theoretical insights for the development of novel therapeutic targets for ND treatment.

Materials and methods

Cell culture and treatment

The renal tubule epithelial cells HK-2 were obtained from the ATCC Cell Bank (Manassas, VA, USA). Cells were cultured in DMEM/F12 medium containing 10% fetal bovine serum and 1% penicillin/streptomycin at 37 °C in a cell culture incubator with 5% CO_2. When the degree of cell fusion reached 70–80%, the cells were incubated in 30 mM glucose-containing medium with HG stimulation for 48 h. The mannitol group (MG) was cultured in 5 mM glucose-containing medium supplemented with 25 mM mannitol.

Cell transfection

Interference and overexpression vectors for P4HB and PRMT1 were constructed by Shanghai Genechem Co., Ltd. (Genechem). The HK-2 cells were seeded into 6-well plates. The cells were transfected with siRNA-P4HB-1/2, siRNA-PRMT1-1/2, Ov-P4HB, Ov-PRMT1, and their corresponding negative control siRNA-NC and Ov-NC using Lipofectamine 2000 (Invitrogen, USA) when the cell confluence reached about 80%. The medium was changed after 6 h, and the cells were cultured in medium with or without HG (30 mM) for 48 h.

Reactive oxygen species (ROS) level detection

Cellular ROS levels were detected using the Reactive Oxygen Species Assay Kit (S0033S, Beyotime). DCFH-DA was diluted to 10 μmol/L. Cell culture medium was removed from six-well plates (1×10^5 cells/well), and 1 mL of diluted DCFH-DA was added when the cells reached 70–80% confluence. Cells were incubated at 37 °C for 20 min, washed three times, and then observed under a laser confocal microscope at an excitation wavelength of 488 nm and an emission wavelength of 525 nm.

Interaction target prediction

The target genes interacting with P4HB were predicted using the Biogrid database (https://thebiogrid.org/). Protein nucleotide sequences in FASTA format were obtained from NCBI database (https://www.ncbi.nlm.nih.gov/). The binding ability of P4HB to PRMT1 was predicted by HDOCK server (http://hdock.phys.hust.edu.cn/).

Immunoprecipitation (IP) assay

HG-induced HK-2 cells were lysed with a cell scraper for 30 min on ice with the addition of lysis buffer containing protease inhibitors and phosphatase inhibitors. Then the cells were centrifugated at 4 ℃ for 15 min at 12,000 rpm, and the supernatant was collected. The protein concentration was determined to be 0.68 μg/μL using the BCA Quantification Kit. 50 μL of protein was taken as Input positive control. Another 400 μL of protein was taken

and added 10 μL of 5 x loading buffer, then the protein were incubated with anti-P4HB, anti-PRMT1, or anti-IgG antibody-coated beads at 4 ℃ for 1 h with shaking. The beads were then washed 3 times with PBS+0.5% Triton and magnetically separated in a metal bath at 95 ℃ for 5 min. Finally, 50 μL of 1x loading buffer was added to magnetic beads or Input samples, and target protein was detected by WB assay.

Western blot assay

The HK-2 cells were lysed on ice for 30 min using a lysate containing protease inhibitors and phosphatase inhibitors. Cells were then centrifuged at 12,000 rpm for 15 min at 4 ℃ and the supernatant was extracted to obtain total protein, which was quantified using the BCA Quantification Kit. 20 μL (14.94 μg) of protein was separated by 10% SDS-PAGE and transferred to a PVDF membrane. The membrane was incubated with primary antibodies overnight at 4 °C. Primary antibodies included PRMT1 antibody (ab190892, 1:1500), P4HB antibody (ab2792, 1:1500), TGF-β antibody (ab179695, 1:5000), SMAD3 antibody (ab40854, 1:1500), p-SMAD3 antibody (ab63403, 1:3000), E-cadherin antibody (AF0131, 1:3000), N-cadherin antibody (AF5239, 1:5000), vimentin antibody (ab92547, 1:1500), α-SMA antibody (AF1032, 1:1500), fibronectin antibody (AF5335, 1:1500), collagen IV antibody (AF0510, 1:2000), SNAIL antibody (AF6032, 1:3000), and SLUG antibody (ab216347, 1:3000). The membrane was washed with TBST and incubated with goat anti-rabbit IgG-HRP (1:2000, ab7090, Abcam) at 37 °C for 2 h. Protein bands were visualized in a developer after dropwise addition of developer solution and quantified using ImageJ. The signal intensities of the target protein and the internal reference protein β-actin in the bands were measured separately using ImageJ to analyze the grayscale values, and then the ratio signal intensities of the target protein to β-actin was calculated to reflect the relative changes in the expression levels of the target protein.

Immunofluorescence assay

The transfected cells were inoculated into 6-well plates, and when the cell fusion reached 70-80%, the cells were fixed with 4% neutral formaldehyde fixative for 30 min at 4℃. Sealing solution was added to each well and incubated at 37 ℃ for 30 min in a constant temperature and humidity incubator. Then diluted primary antibody: N-cadherin (1:200, AF5239), α-SMA (1:200, AF1032) was added and incubated overnight at 4℃. Then diluted goat anti-rabbit IgG H&L (1:200, ab150077, Abcam) was added, and the cells were incubated at room temperature without light for 1 h. After washing the cells with PBS, the nuclei of the cells were re-stained with 4′,6-diamidino-2-phenylindole (DAPI) and observed under a fluorescence microscope.

Enzyme-linked immunosorbent assay (ELISA)

The levels of TGF-β in the supernatant of HK-2 cells was detected using a human TGF-β ELISA kit (PT880, beyotime). HK-2 cells were centrifuged at 2500 rpm for 10 min, and the supernatant was retained. The standard solution and samples were diluted was prepared according to the instructions. Then the standard solution and samples were added to 96-well plates at 100 μL/well and incubated for 2 h at room temperature. After washing, 100 μL of biotinylated antibody was added to each well and incubated for 1 h at room temperature. Then sequentially add 100 μL of horseradish peroxidase-conjugated streptavidin and TMB dye solution and incubate for 20 min at room temperature in the dark. Finally, added 50 μL of termination solution to each well and the A450 value was measured immediately.

Statistical analysis

GraphPad Prism software (version 7.0, USA) was used for statistical analysis. Results represent the mean±standard deviation (SD) values of three independent replicate experiments, and differences between two or more groups were analyzed using Student's t-test or one-way ANOVA. $p<0.05$ was considered statistically significant.

Results

Effect of HG induction on ROS/TGFβ/SMAD3 signaling and P4HB expression in HK-2 cells

Excessive production of ROS may TGFβ/SMAD3 signaling activation through multiple pathways [18, 19]. Therefore, we first investigated ROS levels in HK-2 cells. We observed an increase in the intensity of ROS staining in HK-2 cells in the HG group compared with the control and MG groups (Fig. 1A), suggesting that HG treatment caused an increase in cellular ROS production. Meanwhile, WB results showed that SMAD3 showed no significant changes among control, MG and HG groups. However, compared with the MG group, the expression of TGFβ, phosphorylated SMAD3 (p-SMAD3) and P4HB were significantly increased in HK-2 cells of HG group (Fig. 1B). It indicated that the production of ROS and the activation of TGFβ/SMAD3 signaling were upregulated with increasing glucose concentration.

Interference with P4HB inhibits HG-induced HK-2 cell EMT, fibrosis and TGFβ/SMAD3 signaling

WB assay found that siRNA-P4HB-1 had a better effect of interfering with P4HB expression (Fig. 2A), thus it was selected for further studies. Immunofluorescence results showed that the fluorescence staining intensity of N-cadherin (Fig. 2B) and α-smooth muscle actin (α-SMA)

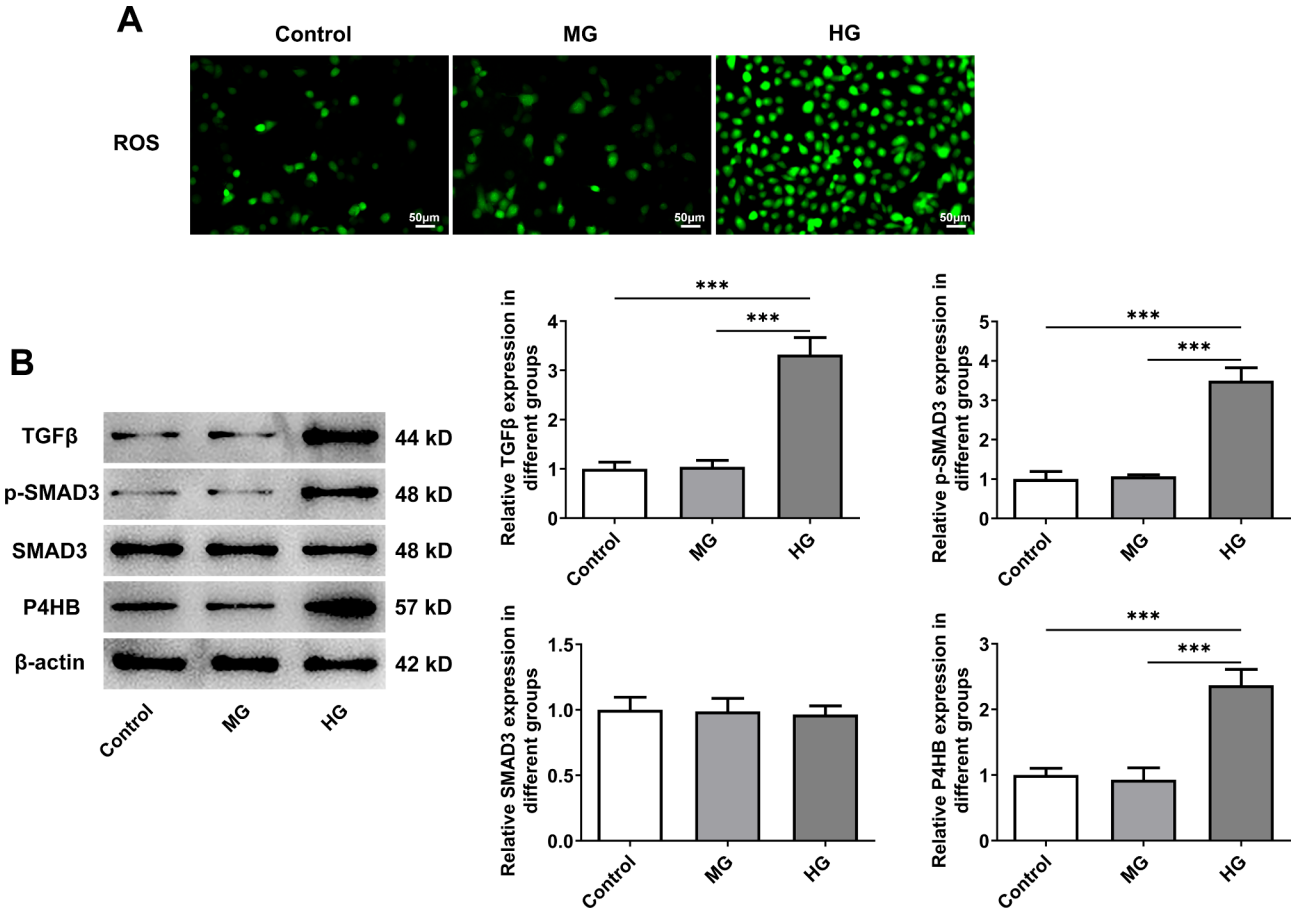

Fig. 1 Effect of HG induction on ROS/TGFβ/SMAD3 signaling and P4HB expression in HK-2 cells. The levels of ROS in HK-2 cells (A, 200 ×); The expression of TGFβ/SMAD3 pathway-related proteins and P4HB in HK-2 cells (B). $n = 3$, *** $P < 0.001$. HK-2, human kidney 2; ROS, Reactive oxygen species; MG, mannitol group; HG, high glucose; TGFβ, transforming growth factor beta 1; SMAD3, SMAD family member 3; p-SMAD3, phosphorylated-SMAD family member 3; P4HB, prolyl 4-hydroxylase subunit beta

(Fig. 2C) was increased after HG induction compared with the control group. WB results showed that the expression of EMT-related protein E-cadherin was decreased, and the expression of N-cadherin and vimentin were increased in the HG group (Fig. 2D). In addition, the expression of fibrosis-related proteins α-SMA, fibronectin and collagen IV was increased in the HG group (Fig. 2E). However, the expression of these proteins was significantly reversed after P4HB interference.

Next, we examined the expression of TGFβ/SMAD3 and its downstream signaling-related proteins. The results showed that HG induction increased the expression of TGFβ, p-SMAD3, SNAIL and SLUG proteins in HK-2 cells. In contrast, TGFβ, p-SMAD3, SNAIL, and SLUG protein expression was decreased after P4HB interference (Fig. 2F). In addition, the levels of TGFβ in the the supernatant of HK-2 cells were increased in the HG group compared with the control group, but was decreased in the HG+si-RNA-P4HB group (Fig. 2G). These results suggest that TGFβ/SMAD3 signaling was upregulated in HK-2 cells of HG group, and P4HB may be involved in HG-induced HK-2 cell mesenchymalization and fibrosis through TGFβ/SMAD3 signaling.

P4HB and PRMT1 bind to each other inHG-induced HK-2 cells

Biogrid database showed that P4HB and PRMT1 had high binding capacity (Supplementary Fig. 1). WB results showed that the expression of PRMT1 was significantly increased in HG-induced HK-2 cells, and the expression of PRMT1 was decreased after interfering with P4HB (Fig. 3A). HDOCK prediction showed that P4HB and PRMT1 were able to interact with each other (Fig. 3B), with a docking score < -200 and a confidence score > 0.7 (Supplementary Fig. 2). IP experimental validation showed that P4HB and PRMT1 were able to bind to each other in HG-induced HK-2 cells (Fig. 3CD).

Interference with PRMT1 attenuates HG-induced HK-2 cell EMT and fibrosis

The study investigated the role of PRMT1 in HG-induced mesenchymalization and fibrosis of renal

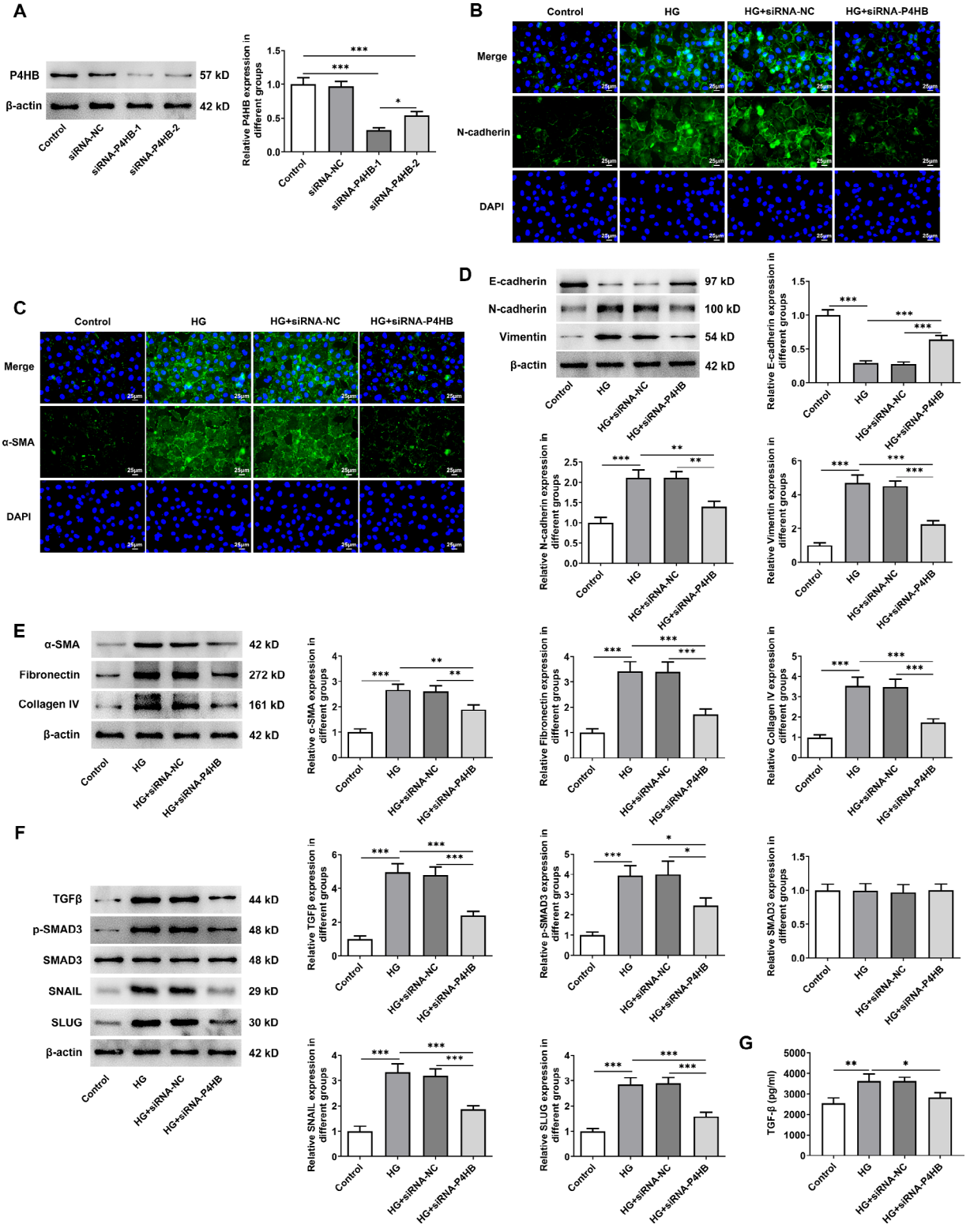

Fig. 2 Interference with P4HB inhibits HG-induced HK-2 cell EMT, fibrosis and TGFβ/SMAD3 signaling. The interference potency of siRNA-P4HB (**A**); The fluorescence intensity of N-cadherin (**B**, 400 ×); The fluorescence intensity of α-SMA (**C**, 400 ×); The expression of EMT-related proteins (**D**). The expression of fibrosis-related proteins (**E**). The expression of TGFβ/SMAD3 signaling-related proteins (**F**). The levels of TGFβ in the supernatant of HK-2 cells (**G**). $n = 3$, * $P < 0.05$, ** $P < 0.01$, *** $P < 0.001$. HK-2, human kidney 2; α-SMA, α-smooth muscle actin; EMT, endothelial mesenchymal transition; HG, high glucose; TGFβ, transforming growth factor beta 1; SMAD3, SMAD family member 3; p-SMAD3, phosphorylated-SMAD family member 3

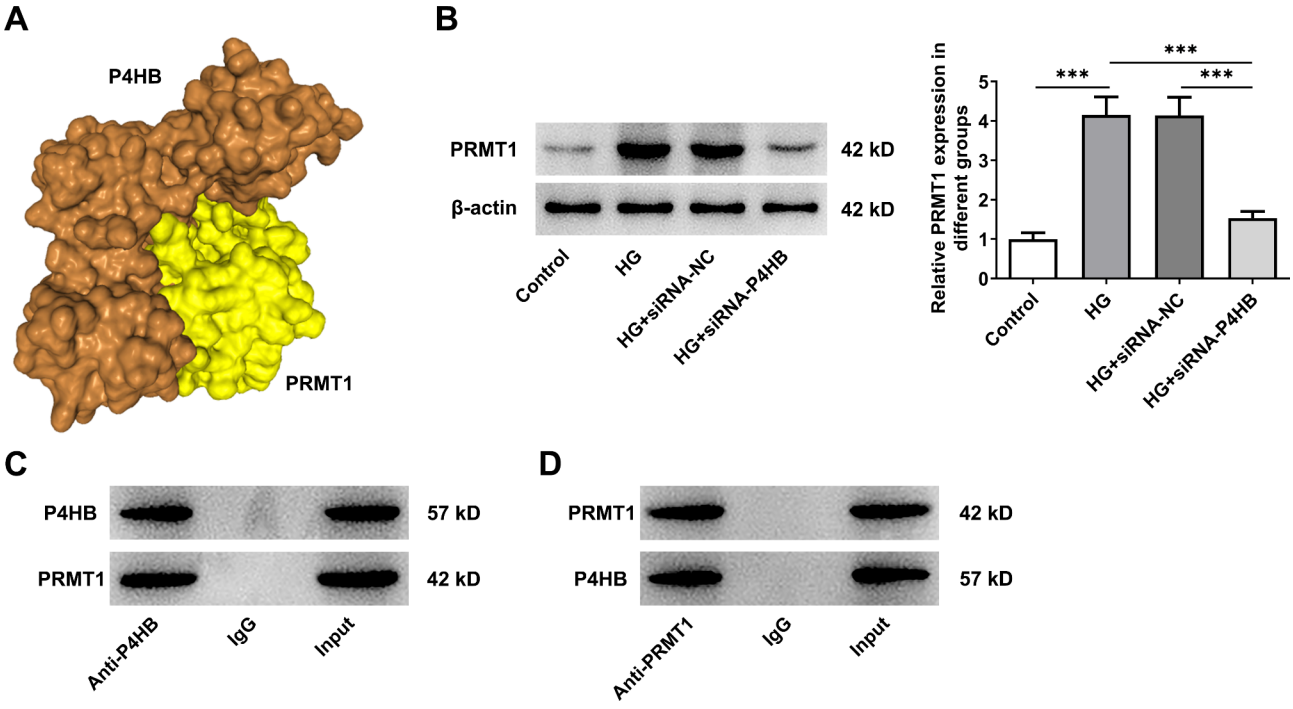

Fig. 3 P4HB and PRMT1 bind to each other in HG-induced HK-2 cells. The expression of PRMT1 in HK-2 cells was detected by WB (**A**). HDOCK predicted P4HB binding to PRMT1 (**B**); Immunoprecipitation (IP) assay to verify P4HB and PRMT1 binding (CD). $n=3$, *** $P<0.001$. HK-2, human kidney 2; HG, high glucose; P4HB, prolyl 4-hydroxylase subunit beta; PRMT1, protein arginine methyltransferase 1

tubular epithelial cells. After screening, the interference plasmid SiRNA-PRMT1-1 was selected for further studies (Fig. 4A). Immunofluorescence results showed that PRMT1 interference suppressed the HG-induced increase in fluorescence intensity of N-cadherin (Fig. 4B) and α-SMA (Fig. 4C). Meanwhile, the expression of EMT-related proteins E-cadherin, N-cadherin, and vimentin (Fig. 4D) and fibrosis-related proteins α-SMA, fibronectin, and collagen IV (Fig. 4E) were significantly reversed after PRMT1 interference, suggesting that PRMT1 is involved in HG-induced EMT and fibrosis of HK-2 cells.

Interference with P4HB attenuates HG-induced HK-2 cell EMT and fibrosis by inhibiting TGFβ/SMAD3 signaling via PRMT1

We investigated the effects of simultaneous transfection of siRNA-PRMT1 and Ov-P4HB on PRMT1 and P4HB expression in HK-2 cells. The results showed that there was no significant difference in P4HB protein expression among HG, HG+SiRNA-NC, HG+siRNA-PRMT1, and HG+siRNA-PRMT1+Ov-NC groups, whereas P4HB protein expression was significantly upregulated in HG+siRNA-PRMT1+Ov-P4HB. In addition, PRMT1 expression was decreased in the HG+siRNA-NC and HG+siRNA-PRMT1 groups, but the expression of PRMT1 was upregulated in HG+siRNA-PRMT1+Ov-P4HB. This suggests that Ov-P4HB was able to promote PRMT1 expression, but siRNA-PRMT1 failed to reduce P4HB expression (Fig. 5A).

Finally, we examined the effect of Ov-PRMT1 on the effect of siRNA-P4HB. Consistent with previous results, the intensity of fluorescent staining of N-cadherin (Fig. 5B) and α-SMA (Fig. 5C) was decreased after interference with P4HB. The expression of E-cadherin was increased, and the expression of N-cadherin, vimentin, α-SMA, fibronectin, and collagen IV was decreased (Fig. 5DE). Additionally, the expression of TGFβ/SMAD3 and its downstream signaling related proteins, TGFβ, p-SMAD3, SNAIL, and SLUG were decreased (Fig. 5F), the levels of TGFβ in the supernatant of HK-2 cells in the HG+siRNA-P4HB group was decreased (Fig. 5G). However, the above effects of siRNA-P4HB were significantly attenuated after PRMT1 overexpression. The above results suggest that the effces of P4HB on TGFβ/SMAD3 signaling, EMT, and fibrosis in HK-2 cells are mediated by PRMT1, while PRMT1 cannot reverse regulate P4HB expression.

Discussion

The stimulation of HG induces EMT and fibrosis in renal tubules, leading to persistent albuminuria, which is a characteristic of DN [20, 21]. This study examined the role of P4HB in HG-induced EMT and fibrosis in renal tubular epithelial cells HK-2. The results showed that HG induced an increase in the expression of P4HB, as well

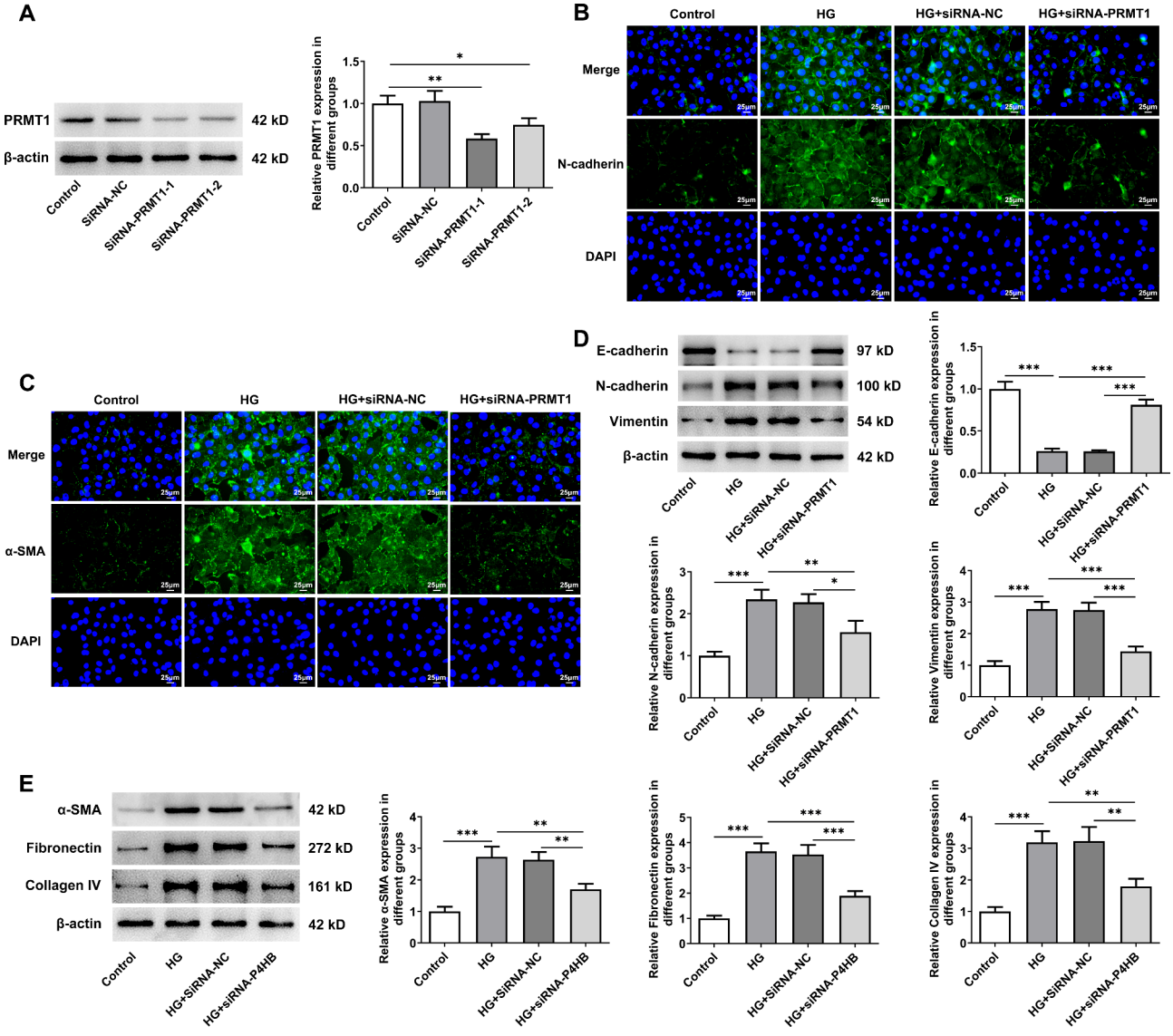

Fig. 4 Interference with PRMT1 attenuates HG-induced HK-2 cell EMT and fibrosis. The interference potency of two siRNA-PRMT1 (**A**); The fluorescence intensity of N-cadherin (**B**, 400 ×); The fluorescence intensity of α-SMA (**C**, 400 ×); The expression of EMT-related proteins (**D**). The expression of fibrosis-related proteins (**E**). $n = 3$, * $P < 0.05$, ** $P < 0.01$, *** $P < 0.001$. HK-2, human kidney 2; α-SMA, α-smooth muscle actin; EMT, endothelial mesenchymal transition; HG, high glucose; PRMT1, protein arginine methyltransferase 1

as proteins associated with EMT and fibrosis in HK-2 cells, and activated the TGFβ/SMAD3 signaling pathway. Interfering with P4HB significantly reduced HG-induced EMT and fibrosis, and inhibited the activation of the TGFβ/SMAD3 signaling pathway. Overexpression of PRMT1, a target of P4HB, reversed the effects of siRNA-P4HB, but siRNA-PRMT1 failed to reduce P4HB expression.

The EMT in renal cells is a prominent manifestation in diabetic nephropathy [22]. Under HG stimulation, renal tubular epithelial cells undergo EMT, abandoning their epithelial characteristics to transform into fibroblasts/myofibroblasts, ultimately leading to interstitial fibrosis of the renal tubules [23, 24]. TGF-β promotes fibrotic progression through binding to receptors and phosphorylating SMAD2/3 [25]. The TGFβ/SMAD3 pathway is the classical signaling pathway in fibrosis, playing a crucial role in mediating the pro-fibrotic response of renal epithelial cells and activating renal fibroblasts [26]. Simultaneously, the fibrotic response is influenced by ROS-mediated TGFβ/SMAD signaling transduction [27]. Consistent with previous findings [28], this study observed elevated ROS levels, increased TGFβ expression, and phosphorylated SMAD3 in HK-2 cells following high glucose induction, indicating activation of the TGFβ/SMAD3 signaling pathway in HK-2 cells.

The study shows an increase in P4HB expression in tubular epithelial cells under HG condition [29]. Likewise,

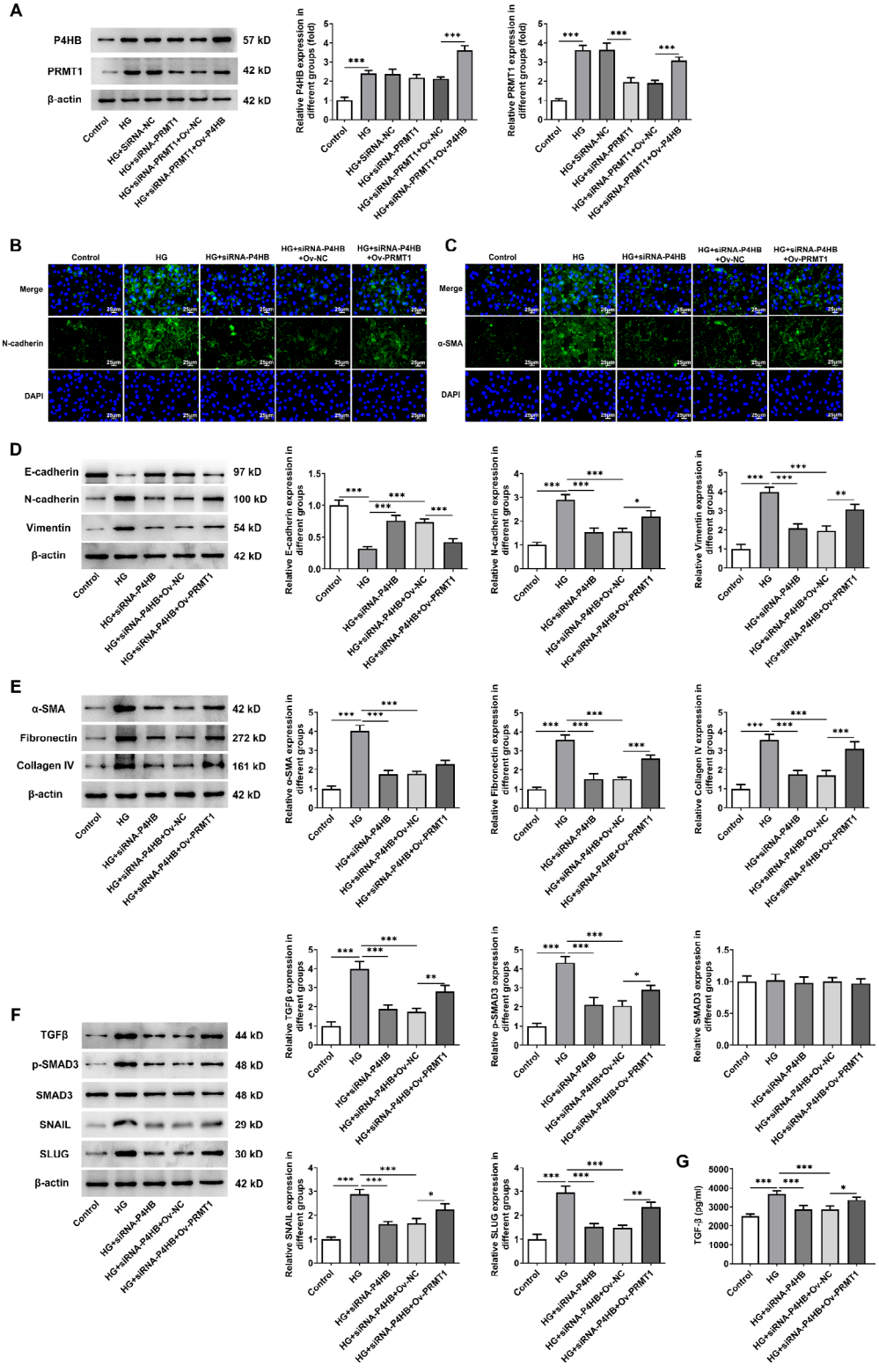

Fig. 5 Interference with P4HB attenuates HG-induced HK-2 cell EMT and fibrosis by inhibiting TGFβ/SMAD3 signaling via PRMT1. The expression of P4HB and PRMT1 (**A**); The fluorescence intensity of N-cadherin (**B, 400 ×**); The fluorescence intensity of α-SMA (**C**, 400 ×); The expression of EMT-related proteins (**D**); The expression of fibrosis-related proteins (**E**). The expression of TGFβ/SMAD3 signaling-related proteins (**F**) The levels of TGFβ in the supernatant of HK-2 cells (**G**). $n = 3$, * $P < 0.05$, ** $P < 0.01$, *** $P < 0.001$. HK-2, human kidney 2; α-SMA, α-smooth muscle actin; EMT, endothelial mesenchymal transition; HG, high glucose; TGFβ, transforming growth factor beta 1; SMAD3, SMAD family member 3; p-SMAD3, phosphorylated-SMAD family member 3; SNAIL, snail family transcriptional repressor 1; SLUG, snail family transcriptional repressor 2

this research notes an elevation of P4HB expression in HK-2 cells induced by HG. Following that, the study explores the function of P4HB in HK-2 cells induced by HG. E-cadherin and N-cadherin, as members of the cadherin family, are vital for preserving tissue structural integrity [15]. The reduction in E-cadherin expression coupled with a simultaneous rise in N-cadherin is recognized as characteristic of EMT [30]. Moreover, in EMT, increased Vimentin expression and its staining act as indicators for cells from the interstitium or experiencing EMT [31]. Fibrosis arises due to the excessive buildup of extracellular matrix elements including collagen, fibronectin, and α-SMA [32]. This study demonstrated that after exposure to HG, there was a decline in E-cadherin expression alongside an elevation in N-cadherin and Vimentin within HK-2 cells. Concurrently, HG condition increased the expression of fibrosis-related proteins such as α-SMA, Fibronectin, and Collagen IV in HK-2 cells. This implies that HG induce EMT and fibrosis in HK-2 cells. However, interfering with P4HB reversed the mentioned changes induced by HG. This suggests that interfering with P4HB inhibited EMT and fibrosis in HK-2 cells exposed to HG.

Through online database queries and in vitro experiments, we have validated the combining capacity of P4HB and PRMT1. It has been reported that the expression of PRMT1 in the serum of DN patients and in the renal tissues of DN mice was increased. HG induction in HK-2 cells results in increased PRMT1 expression, coupled with endoplasmic reticulum stress and activation of EMT [31]. This implies that PRMT1 might contribute to the development of EMT and fibrosis in DN. In line with prior research, we observe an upregulation of PRMT1 expression in HK-2 cells treated with HG in this study. Interfering with PRMT1 markedly counteracted the expression of EMT and fibrosis related proteins in HK-2 cells induced by HG, which is consist with the effects of P4HB interference. To confirm whether P4HB affects HG-induced EMT and fibrosis in HK-2 cells by mediating PRMT1, we co-transfected siRNA-P4HB and Ov-PRMT1 into HK-2 cells. The findings suggested that PRMT1 overexpression mitigates the regulatory effect of P4HB interference on the expression of E-cadherin, N-cadherin, Vimentin, α-SMA, Fibronectin, Collagen IV, TGFβ, p-SMAD3, SNAIL, and SLUG. This implies that the effect of P4HB on EMT and fibrosis in HK-2 cells was mediated by PRMT1.

Although current research confirms that P4HB regulates the TGFβ/SMAD3 signaling pathway through PRMT1 to inhibit HG-induced EMT and fibrosis in HK-2 cells, there are still some limitations in the current study. Firstly, this research was mainly conducted in HK-2 cells, and in vivo experiments often cannot replicate the true environment of the body. Renal proximal tubular epithelial cells (RPTEC) are renal proximal tubular epithelial cells that better preserve various physiological functions and characteristics of primary cells. Therefore, the same experimental design can be conducted in RPTEC cells to further support the findings of the current study. Moreover, the regulatory role of P4HB in EMT and fibrosis in ND needs to be validated through animal experiments.

In summary, this study elucidated the role of P4HB in HG-induced EMT and fibrosis in HK-2 cells through in vitro experiments. The results indicated that P4HB regulates the TGFβ/SMAD3 signaling pathway by mediating PRMT1, thereby contributing to HG-induced tubular epithelial cell EMT and fibrosis.

Supplementary Information

The online version contains supplementary material available at https://doi.org/10.1186/s12882-024-03733-5.

Supplementary Material 1: **Supplementary Fig. 1**. The targets that interacted with P4HB were predicted by the Biogrid database.

Supplementary Material 2: **Supplementary Fig. 2**. Parameters of HDOCK predicting P4HB and PRMT1 binding.

Acknowledgements
Not appropriate.

Author contributions
Haifeng Wang: Experiment, Sample collection, Data curation, Writing – original draft; Yang Li: Experiment, Investigation, Data curation, Writing original draft; Na Wu: Experiment, Data curation, Data analysis; Chunmei Lv: Investigation, Data curation, Funding; Yishu Wang: Experimental design, supervision, Writing – review & editing.

Funding
Hypoxia conditioning medicine (The key supporting specialty of Beijing Medical Management Center ZYLX202138).

Data availability
Data is provided within the manuscript or supplementary information files.

Declarations

Ethical approval and consent to participate
Not applicable.

Competing interests
The authors declare no competing interests.

Received: 19 March 2024 / Accepted: 26 August 2024
Published online: 09 September 2024

References

1. Global, regional, and national burden of chronic kidney disease, 1990–2017: a systematic analysis for the Global Burden of Disease Study 2017. Lancet. 2020;395(10225):709–33.
2. Samsu N. Diabetic Nephropathy: challenges in Pathogenesis, diagnosis, and treatment. Biomed Res Int. 2021;2021:p1497449.
3. Permyakova A, et al. A Novel Indoline Derivative ameliorates Diabesity-Induced chronic kidney disease by reducing metabolic abnormalities. Front Endocrinol (Lausanne). 2020;11:91.

4. Miyata T, Suzuki N. Ypersele De Strihou, Diabetic nephropathy: are there new and potentially promising therapies targeting oxygen biology?. Kidney Int. 2013;84(4):693–702. van.
5. Xiao L, et al. A glimpse of the pathogenetic mechanisms of Wnt/β-catenin signaling in diabetic nephropathy. Biomed Res Int. 2013;2013:987064.
6. Ma Z, et al. Berberine protects diabetic nephropathy by suppressing epithelial-to-mesenchymal transition involving the inactivation of the NLRP3 inflammasome. Ren Fail. 2022;44(1):923–32.
7. Mohamed R, et al. Low-dose IL-17 Therapy prevents and reverses Diabetic Nephropathy, metabolic syndrome, and Associated Organ Fibrosis. J Am Soc Nephrol. 2016;27(3):745–65.
8. Sharma S et al. E4 engages uPAR and enolase-1 and activates urokinase to exert antifibrotic effects. JCI Insight, 2021, 6(24).
9. Choi JH et al. Platyconic Acid A, Platycodi Radix-Derived Saponin, suppresses TGF-1-induced activation of hepatic stellate cells via blocking SMAD and activating the PPAR signaling pathway. Cells, 2019, 8(12).
10. Zhang T, et al. Super-enhancer hijacking LINC01977 promotes malignancy of early-stage lung adenocarcinoma addicted to the canonical TGF-β/SMAD3 pathway. J Hematol Oncol. 2022;15(1):114.
11. Lin HC, et al. Glycyrrhiza uralensis root extract ameliorates high glucose-induced renal proximal tubular fibrosis by attenuating tubular epithelial-myofibroblast transdifferentiation by targeting TGF-β1/Smad/Stat3 pathway. J Food Biochem. 2022;46(5):e14041.
12. Hao Y, Baker D, Ten Dijke P. TGF-β-Mediated epithelial-mesenchymal transition and Cancer metastasis. Int J Mol Sci, 2019, 20(11).
13. De Bessa TC, et al. Subverted regulation of Nox1 NADPH oxidase-dependent oxidant generation by protein disulfide isomerase A1 in colon carcinoma cells with overactivated KRas. Cell Death Dis. 2019;10(2):143.
14. Hazari Y, et al. The endoplasmic reticulum stress sensor IRE1 regulates collagen secretion through the enforcement of the proteostasis factor P4HB/PDIA1 contributing to liver damage and fibrosis. bioRxiv; 2023.
15. Bai F, et al. Identification and validation of P4HB as a novel autophagy-related biomarker in diabetic nephropathy. Front Genet. 2022;13:965816.
16. Chen YY, et al. Protein arginine methyltranferase-1 induces ER stress and epithelial-mesenchymal transition in renal tubular epithelial cells and contributes to diabetic nephropathy. Biochim Biophys Acta Mol Basis Dis. 2019;1865(10):2563–75.
17. Wei H, et al. Protein arginine methyltransferase 1 promotes epithelial-mesenchymal transition via TGF-β1/Smad pathway in hepatic carcinoma cells. Neoplasma. 2019;66(6):918–29.
18. Lee JH, et al. Endoplasmic reticulum stress activates transglutaminase 2 leading to protein aggregation. Int J Mol Med. 2014;33(4):849–55.
19. Zeigler AC, et al. A computational model of cardiac fibroblast signaling predicts context-dependent drivers of myofibroblast differentiation. J Mol Cell Cardiol. 2016;94:72–81.
20. Lu Q, et al. Inactivation of TSC1 promotes epithelial-mesenchymal transition of renal tubular epithelial cells in mouse diabetic nephropathy. Acta Pharmacol Sin. 2019;40(12):1555–67.
21. Zhao L, et al. LncRNA KCNQ1OT1 promotes the development of diabetic nephropathy by regulating miR-93-5p/ROCK2 axis. Diabetol Metab Syndr. 2021;13(1):108.
22. Liu Z, et al. Endoplasmic reticulum stress-triggered ferroptosis via the XBP1-Hrd1-Nrf2 pathway induces EMT progression in diabetic nephropathy. Biomed Pharmacother. 2023;164:114897.
23. Loeffler I, Wolf G. Epithelial-to-mesenchymal transition in Diabetic Nephropathy: fact or fiction? Cells. 2015;4(4):631–52.
24. Zhang J, et al. Glutathione prevents high glucose-induced pancreatic fibrosis by suppressing pancreatic stellate cell activation via the ROS/TGFβ/SMAD pathway. Cell Death Dis. 2022;13(5):440.
25. Sun B et al. Hippuric Acid promotes renal fibrosis by disrupting Redox Homeostasis via Facilitation of NRF2-KEAP1-CUL3 interactions in chronic kidney disease. Antioxid (Basel), 2020, 9(9).
26. Hernández-Aquino E, et al. Naringenin prevents experimental liver fibrosis by blocking TGFβ-Smad3 and JNK-Smad3 pathways. World J Gastroenterol. 2017;23(24):4354–68.
27. Ren Q, et al. Natural flavonoid pectolinarigenin alleviated Hyperuricemic Nephropathy via suppressing TGFβ/SMAD3 and JAK2/STAT3 signaling pathways. Front Pharmacol. 2021;12:792139.
28. Gong EY et al. VSIG4 induces Epithelial-Mesenchymal Transition of Renal Tubular Cells under high-glucose conditions. Life (Basel), 2020, 10(12).
29. Loh CY et al. The E-Cadherin and N-Cadherin switch in Epithelial-To-Mesenchymal transition: signaling, therapeutic implications, and challenges. Cells, 2019, 8(10).
30. Ko H, et al. Phosphorylation-dependent stabilization of MZF1 upregulates N-cadherin expression during protein kinase CK2-mediated epithelial-mesenchymal transition. Oncogenesis. 2018;7(3):27.
31. Zhao S, et al. Selective deletion of MyD88 signaling in α-SMA positive cells ameliorates experimental intestinal fibrosis via post-transcriptional regulation. Mucosal Immunol. 2020;13(4):665–78.
32. Zelenko Z, et al. Silencing vimentin expression decreases pulmonary metastases in a pre-diabetic mouse model of mammary tumor progression. Oncogene. 2017;36(10):1394–403.

Publisher's note